

Do Understanding and Generation Fight? A Diagnostic Study of DPO for Unified Multimodal Models

Abinav Rao

Sujan Rachuri

Abstract

Unified multimodal models share a language model backbone for both understanding and generating images. Can DPO align both capabilities simultaneously? We present the first systematic study of this question, applying DPO to Janus-Pro at 1B and 7B parameters under seven training strategies and two post-hoc methods. The central finding is negative: generation quality resists DPO alignment across all tested conditions on this architecture. No method improves generation CLIPScore at 7B ($|\Delta| < 0.2$, $p > 0.5$ at $n=200$ per seed, 3 seeds); at 1B, all methods degrade generation, and the result holds across preference data types (real-vs-generated and model-vs-model) and the data volumes tested (150–288 pairs). Gradient analysis reveals why: understanding and generation gradients are near-orthogonal ($\cos \approx 0$) with $\sim 11\text{--}14\times$ magnitude imbalance driven by VQ token count asymmetry (576 generation tokens vs. $\sim 30\text{--}100$ text tokens). This imbalance is the dominant interference mechanism in multi-task DPO; magnitude-balancing yields directionally positive understanding deltas ($+0.01\text{--}0.04$ VQA, though individually not significant), but the generation gap persists regardless. We identify discrete VQ tokenization as a likely structural bottleneck—supported by the generation DPO loss converging to $\ln 2$ —and provide practical guidance for practitioners working with VQ-based unified models.

1. Introduction

A new class of multimodal models can both understand and generate images within a single architecture [2, 3, 25, 26, 28, 29, 31, 37]. This unification is powerful, but it creates a problem when we try to align both capabilities with human preferences. Prior work applies DPO [19] to multimodal understanding [21, 24, 32, 34] or to image generation [23], but always *one modality at a time*. No prior work has applied DPO to both capabilities simultaneously. The obstacle is fundamental: both tasks share a language model backbone, so optimizing for better visual question answering perturbs the same parameters responsible for generation quality, and vice versa, creating a *multi-objective alignment*

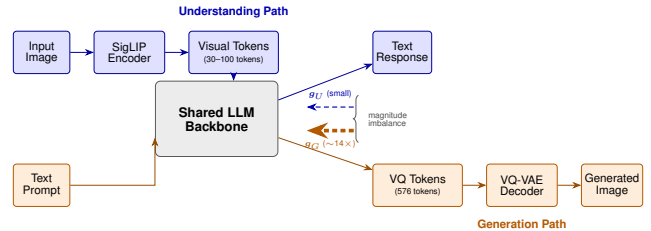


Figure 1. **Janus-Pro architecture and gradient imbalance.** The understanding path (blue) encodes images via SigLIP into visual tokens and produces text responses ($\sim 30\text{--}100$ tokens), while the generation path (orange) decodes 576 VQ tokens through a VQ-VAE. Both paths share the LLM backbone (gray). During multi-task DPO, generation gradients g_G are $\sim 14\times$ larger than understanding gradients g_U (dashed arrows, thickness proportional to magnitude), drowning out the understanding signal in the shared parameters.

problem (Figure 1).

A natural hypothesis is that the two objectives produce *conflicting* gradients, pushing shared parameters in opposing directions. We test this directly through gradient analysis on Janus-Pro [3] at two scales (1B and 7B parameters). The study yields four key findings:

- 1. Generation quality resists DPO alignment.** No method out of seven training strategies and two post-hoc methods improves generation CLIPScore at $n=200$ per seed across 3 seeds ($p > 0.5$). The result holds with real-vs-generated preference data, model-vs-model preference data (Appendix H), and across data scales from 150 to 288 pairs (Appendix I), pointing to a structural bottleneck in Janus-Pro’s discrete VQ tokenization.
- 2. The interference mechanism is magnitude imbalance.** Understanding and generation DPO gradients are near-orthogonal ($\cos \approx 0$), occupying separate subspaces. Generation gradients are $\sim 11\text{--}14\times$ larger because generation operates over 576 VQ tokens versus $\sim 30\text{--}100$ text tokens, drowning out the understanding signal (§4.2).
- 3. Magnitude correction preserves understanding in multi-task DPO.** Dynamic gradient reweighting converges to $w_U \approx 0.93$, approximately matching the ana-

lytical sequence-length ratio $N/(N+T) \approx 0.92$; setting this ratio as a fixed weight produces equivalent results. All three magnitude-balancing approaches show positive VQA deltas (+0.01–0.04) during multi-task training at 7B—directionally consistent but individually not statistically significant ($p > 0.6$)—while PCGrad [33] and naive joint DPO do not (§4.3).

4. **The diagnostic generalizes across model scales.** Both 1B and 7B exhibit the same gradient dynamics (magnitude ratios $\rho = 0.07\text{--}0.09$, *i.e.*, 11–14 \times generation dominance), tracing to the architecture-level VQ token count, which is scale-invariant (§4.4).

In summary, we contribute: (i) a negative result showing that offline DPO cannot improve generation quality in Janus-Pro’s VQ-based architecture, robust across seven training strategies and two post-hoc methods, two data construction methods, the data volumes tested, two model sizes, and three random seeds; (ii) a gradient-level diagnosis identifying magnitude imbalance as the dominant interference mechanism, with null-hypothesis calibration consistent with genuine orthogonality; (iii) practical guidance: understanding-only DPO is safe and effective, magnitude-balancing preserves these gains in multi-task settings, and generation improvement likely requires on-policy methods or continuous-representation architectures.

2. Related Work

Unified Multimodal Models. Chameleon [2] introduced early-fusion token-based mixed-modal generation; Transfusion [37] combined autoregressive text with continuous diffusion in a shared transformer. Janus [26] and Janus-Pro [3] decouple visual encoders (SigLIP for understanding, VQ-VAE for generation) while sharing only the LLM backbone. Emu3 [25] matches diffusion-model quality with purely autoregressive prediction; Show-o [29] blends autoregressive text with discrete diffusion. BLIP3-o [28] and MMaDA [31] manage understanding-generation trade-offs during *pretraining* via decoupled encoders, sequential training, or online RL. None of these works study how the two capabilities interact during *offline preference optimization*, the setting we address.

DPO for Multimodal Understanding and Generation.

Preference optimization for vision-language understanding includes factually augmented RLHF [21], RLHF-V [34], RLAI-F-V [35], mDPO [24], and OPA-DPO [32]. For generation, Diffusion-DPO [23] reformulated DPO for diffusion models, while ImageReward [30] and HPS v2 [27] provide learned reward models. Every existing method optimizes *one modality in isolation*. We study what happens when both are optimized simultaneously through a shared backbone.

Multi-Objective Alignment and the Alignment Tax.

Tension between alignment objectives is well-documented [17]. Safe RLHF [6] decouples helpfulness from harmlessness via Lagrangian optimization. Rewarded Soups [20] exploits linear mode connectivity for Pareto-optimal interpolation. Lin *et al.* [16] show that RLHF causes capability forgetting (the *alignment tax*). NSPO [5] projects safety gradients into the null space of task representations to avoid first-order degradation. In multi-task learning, GradNorm [4] balances task weights by gradient magnitudes, and PCGrad [33] projects conflicting gradients onto normal planes. Concurrent work applies *online* RL to unified models: UniGRPO (from MMaDA) [31] and UniRL-Zero [36] use reward-model-based reinforcement learning, requiring on-policy generation. We take the complementary *offline* approach via DPO and find that, for VQ-based unified models, offline preference optimization cannot improve generation quality at all, while magnitude-balancing is sufficient to protect understanding gains in multi-task settings.

3. Method

We first formalize multi-task DPO for unified models (§3.1), then develop the gradient analysis framework that reveals the magnitude imbalance (§3.2), describe magnitude-balancing corrections (§3.3), and list all comparison methods (§3.4).

3.1. DPO for Unified Models

Preliminaries. Direct Preference Optimization [19] aligns a policy π_θ with human preferences using a dataset of preference triples $\mathcal{D} = \{(x^{(i)}, y_w^{(i)}, y_l^{(i)})\}_{i=1}^N$, where y_w is preferred over y_l given context x . The DPO loss is:

$$\mathcal{L}_{\text{DPO}}(\theta) = -\mathbb{E}_{(x, y_w, y_l) \sim \mathcal{D}} [\log \sigma(\beta \Delta_\theta(x, y_w, y_l))] \quad (1)$$

where σ is the logistic function, $\beta > 0$ is a temperature parameter controlling deviation from the reference policy π_{ref} , and

$$\Delta_\theta(x, y_w, y_l) = \log \frac{\pi_\theta(y_w|x)}{\pi_{\text{ref}}(y_w|x)} - \log \frac{\pi_\theta(y_l|x)}{\pi_{\text{ref}}(y_l|x)} \quad (2)$$

is the difference in implicit rewards between the chosen and rejected responses.

Understanding DPO. For visual understanding, $x = (\mathbf{I}, q)$ is an image-question pair and $y = (y_1, \dots, y_T)$ is a text response. The log-probability decomposes autoregressively:

$$\log \pi_\theta(y|\mathbf{I}, q) = \sum_{t=1}^T \log p_\theta(y_t | y_{<t}, \mathbf{I}, q) \quad (3)$$

Generation DPO. For image generation in autoregressive VQ-based models, x is a text prompt and $y = (v_1, \dots, v_N)$ is a sequence of discrete visual tokens:

$$\log \pi_\theta(y|x) = \sum_{t=1}^N \log p_\theta(v_t | v_{<t}, x) \quad (4)$$

where $N = 576$ for Janus-Pro (24×24 spatial tokens from a VQ-VAE with codebook size $C = 16,384$). The 576-token generation sequence creates a fundamental asymmetry: because $N \gg T$, the generation log-probability sums over $6\text{--}19 \times$ more terms than understanding. As we show in §4.2, this token-count asymmetry is the dominant factor in the observed gradient magnitude imbalance. The measured $\sim 14 \times$ ratio ($1/\rho = 1/0.073$) exceeds the pure token-count ratio ($576/65 \approx 9 \times$, using the mean text length); the residual factor likely reflects higher per-token gradient magnitudes for VQ codebook entries, consistent with the smaller VQ codebook (16,384 vs. $\sim 32,000$ text vocabulary) concentrating probability mass over fewer entries.

Multi-task DPO. Given understanding preferences $\mathcal{D}_U = \{(I_i, q_i, y_{w,i}, y_{l,i})\}$ and generation preferences $\mathcal{D}_G = \{(x_j, I_{w,j}, I_{l,j})\}$, the naive joint objective is:

$$\mathcal{L}_{\text{joint}}(\theta) = \alpha \mathcal{L}_{\text{DPO}}^U(\theta) + (1 - \alpha) \mathcal{L}_{\text{DPO}}^G(\theta) \quad (5)$$

with fixed $\alpha = 0.5$. This equal weighting ignores the gradient magnitude asymmetry identified above. As we show empirically, it fails to preserve understanding gains during multi-task training.

3.2. Gradient Analysis Framework

Let θ_s denote the shared parameters of the unified model’s LLM backbone. In our case, θ_s comprises the LoRA adapters applied to all transformer layers; the task-specific generation head is excluded as it does not participate in multi-task interference. Define the task-specific gradients:

$$\mathbf{g}_U = \nabla_{\theta_s} \mathcal{L}_{\text{DPO}}^U, \quad \mathbf{g}_G = \nabla_{\theta_s} \mathcal{L}_{\text{DPO}}^G \quad (6)$$

We characterize the gradient interaction along two complementary axes:

Directional alignment. The cosine similarity $\cos(\mathbf{g}_U, \mathbf{g}_G) = \frac{\mathbf{g}_U \cdot \mathbf{g}_G}{\|\mathbf{g}_U\| \|\mathbf{g}_G\|}$ measures whether tasks push shared parameters in the same ($\cos > 0$), opposing ($\cos < 0$), or orthogonal ($\cos \approx 0$) directions.

Magnitude ratio. The ratio $\rho = \|\mathbf{g}_U\| / \|\mathbf{g}_G\|$ captures scale imbalance. When $\cos(\mathbf{g}_U, \mathbf{g}_G) = 0$ and $\rho \ll 1$, the combined gradient is dominated by \mathbf{g}_G :

$$\frac{\|\mathbf{g}_U + \mathbf{g}_G\| - \|\mathbf{g}_G\|}{\|\mathbf{g}_G\|} \approx \frac{1}{2} \rho^2 \quad \text{when } \cos = 0, \rho \ll 1 \quad (7)$$

Understanding contributes *quadratically* less as ρ shrinks, and the combined gradient deviates from \mathbf{g}_G by only $\arctan(\rho) \approx \rho$ radians (5.7° for $\rho = 0.1$).

We compute both metrics per mini-batch and per layer (§4.2).

3.3. Gradient-Weighted Balanced DPO

The analysis above identifies magnitude imbalance as the operative interference mechanism. The fix follows directly: adjust task weights to equalize gradient contributions. We test three corrections; the dynamic variant, following Grad-Norm [4], sets:

$$w_U = \frac{\|\mathbf{g}_G\|}{\|\mathbf{g}_U\| + \|\mathbf{g}_G\|}, \quad w_G = \frac{\|\mathbf{g}_U\|}{\|\mathbf{g}_U\| + \|\mathbf{g}_G\|} \quad (8)$$

so that each task’s *weighted* gradient contribution is equalized:

$$w_U \|\mathbf{g}_U\| = w_G \|\mathbf{g}_G\| = \frac{\|\mathbf{g}_U\| \cdot \|\mathbf{g}_G\|}{\|\mathbf{g}_U\| + \|\mathbf{g}_G\|} \quad (9)$$

The balanced loss $\mathcal{L}_{\text{balanced}} = w_U \mathcal{L}_{\text{DPO}}^U + w_G \mathcal{L}_{\text{DPO}}^G$ recomputes weights every K steps to amortize the cost of dual backward passes. When $\|\mathbf{g}_G\| \gg \|\mathbf{g}_U\|$ (the regime we observe), $w_U \rightarrow 1$ and $w_G \rightarrow 0$, amplifying the under-represented understanding signal.

3.4. Comparison Methods

Each comparison method embodies a different assumption about the gradient interaction, so together they form a diagnostic suite. We compare gradient-weighted Balanced DPO against six other training configurations and two post-hoc methods:

Single-task DPO. Understanding-only and generation-only DPO, each trained on their respective preference data. These establish the single-task alignment tax and provide LoRA weights for Rewarded Soups.

Naive joint DPO. Equal-weighted ($\alpha = 0.5$) combination of both losses (Equation (5)).

PCGrad [33]. When $\cos(\mathbf{g}_U, \mathbf{g}_G) < 0$, each gradient is projected onto the normal plane of the other to remove conflicting components; non-conflicting gradients pass through unmodified.

Rewarded Soups [20]. We train understanding-only and generation-only LoRA adapters separately, then interpolate $\theta_s^{\text{soup}} = (1-\lambda) \theta_s^U + \lambda \theta_s^G$ for $\lambda \in \{0.3, 0.5, 0.7\}$.

Separate LoRA adapters. A non-deployable composite oracle: understanding metrics from the understanding-only LoRA, generation metrics from the generation-only LoRA, requiring task-identity knowledge and two adapters at inference time.

Static-weight ablations. Length-normalized: $w_U = N/(N+T) \approx 0.92$, $w_G \approx 0.08$ from sequence lengths. **Fixed-weight:** $w_U = 0.93$, $w_G = 0.07$, matching gradient-weighted convergence.

Beta ablation. We sweep $\beta \in \{0.05, 0.1, 0.2, 0.5\}$ for gradient-weighted Balanced DPO to test sensitivity.

4. Experiments

4.1. Setup

Models. We use Janus-Pro at two scales, **7B** and **1B** parameters [3], both sharing a DeepSeek-LLM [7] backbone with decoupled visual encoders (SigLIP-Large-Patch16-384 for understanding, VQ-VAE with codebook size 16,384 and 576 tokens per image for generation). Decoupled encoders isolate modality-specific processing, making Janus-Pro an ideal testbed: any gradient interference must originate in the *shared backbone*. Evaluating at two scales tests whether gradient dynamics are structural or scale-dependent.

We apply LoRA [12] (rank 64, $\alpha = 128$, dropout 0.05) to all projection matrices (q, k, v, o , gate, up, down) in the language model backbone. Visual encoders are frozen; the generation head (mapping LLM hidden states to VQ codebook logits) remains trainable.

Preference Data. We construct preference pairs for both tasks from COCO val2017 [15]:

- **Understanding** (1,300 pairs): For COCO val2017 images, we pose diverse VQA questions and generate two responses using different prompt formulations. Responses are scored by content overlap with COCO ground-truth captions (penalizing short/degenerate outputs and rewarding novel factual content). Pairs with score margin < 0.5 are filtered out.
- **Generation** (288 pairs): For ~ 400 COCO captions as prompts, we use the *real COCO photograph* as the chosen image and a model-generated image as the rejected image, verified by CLIP-ViT-B/32 [18] text-image similarity. Only pairs where the real image scores higher are retained.

Training. All experiments use DPO temperature $\beta = 0.1$ (unless stated otherwise), learning rate 1×10^{-6} with

AdamW (weight decay 0.01), cosine learning rate schedule, gradient clipping at norm 1.0, and 1,000 training steps with batch size 1 (chosen for per-sample gradient analysis; the 576-token generation sequences also constrain memory at larger batch sizes). Gradient weights (Equation (8)) are recomputed every $K = 50$ steps. With 288 generation pairs and 1,000 steps at batch size 1, each generation pair is seen ~ 3.5 times; with 1,300 understanding pairs, each is seen ~ 0.77 times. For single-task conditions, each task uses all 1,000 steps on its own dataset. Janus-Pro-7B runs on a single NVIDIA H100 80GB; Janus-Pro-1B on a single A100 40GB.

Evaluation. We evaluate each trained model on three dimensions:

- **Understanding:** VQA score (200 held-out samples; scale 0–6) computed as the count of ground-truth COCO caption entities correctly mentioned in the model’s response, penalizing degenerate short outputs.
- **Generation:** CLIPScore using CLIP-ViT-L/14 [18] (200 generated images, near-deterministic decoding at temperature 0.1), deliberately different from the CLIP-ViT-B/32 used in data construction to avoid circular evaluation.
- **Hallucination:** POPE-style [14] yes/no questions ($n \approx 80$ valid responses per condition after discarding unparseable answers); results are degenerate (F1 = 0.0 across all conditions) and reported in Appendix F.

4.2. Gradient Analysis

We compute understanding and generation DPO gradients on shared LoRA parameters across 200 independent mini-batches (each a single preference pair, providing 200 independent gradient samples) at both model scales, using the base (pre-DPO) model. All training experiments are repeated over 3 random seeds. The results reveal an unexpected gradient landscape: near-orthogonality with extreme magnitude imbalance. Training dynamics (Figure 3) confirm these properties persist throughout 1,000 steps of DPO.

Gradients are near-orthogonal. Figure 2 (left) shows the distribution of cosine similarities between g_U and g_G . For Janus-Pro-7B, mean cosine similarity is $-0.0001 (\pm 0.0029)$, with 47.5% of batches negative, exactly what one expects for orthogonal vectors in high-dimensional space. Janus-Pro-1B shows weak anti-alignment (mean cosine = -0.003 , 79.8% negative batches), suggesting mild conflict at smaller scale. At both scales, cosine magnitudes are below 0.004, well within the range expected for orthogonal vectors in high-dimensional space.

Null hypothesis calibration. To confirm that near-zero inter-task cosine reflects genuine orthogonality, we com-

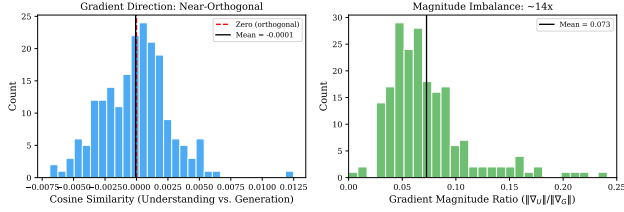


Figure 2. **Gradient diagnostics for Janus-Pro-7B** (200 mini-batches). **Left:** Cosine similarity between understanding and generation gradients. Values center at zero, confirming that the gradients are near-orthogonal and occupy separate subspaces. **Right:** Magnitude ratio $\|g_U\|/\|g_G\|$. Generation gradients are $\sim 14\times$ larger, starving the understanding signal under equal weighting. Janus-Pro-1B shows qualitatively identical magnitude imbalance with slight anti-alignment (mean cosine = -0.003).

pute *intra-task* cosines between consecutive mini-batches as a calibration baseline. Intra-understanding cosine is $+0.040$ (± 0.061) and intra-generation is $+0.006$ (± 0.033), both significantly above the inter-task value of -0.0001 (Welch’s $t = 9.37$, $p < 10^{-17}$ and $t = 2.72$, $p = 0.007$, respectively). Gradients within each task occupy coherent subspaces; the near-zero inter-task cosine reflects genuine structural orthogonality (Appendix B.1).

Magnitude imbalance drives interference. Figure 2 (right) reveals the dominant mechanism. The magnitude ratio $\rho = \|g_U\|/\|g_G\|$ is 0.073 for 7B ($1/\rho \approx 14\times$) and 0.093 for 1B ($1/\rho \approx 11\times$); generation gradients dominate by over an order of magnitude. The cause is sequence length asymmetry: generation DPO operates over $N = 576$ VQ tokens per image versus $T \approx 30\text{--}100$ text tokens, producing proportionally more gradient signal through the summed log-probability (Equation (4)). Under equal-weighted training (Equation (5)), understanding contributes only $\rho/(1 + \rho) \approx 7\%$ of the combined gradient norm, effectively starved of learning signal.

Per-layer analysis. Per-layer gradient cosine similarity across all 30 transformer layers fluctuates around zero at every depth with no systematic trend (Appendix B.3), confirming that orthogonality is uniform across all layers.

4.3. Multi-Task DPO Results

Table 1 presents results across all conditions (3 random seeds, $n=200$ per seed), evaluated with near-deterministic generation (temperature 0.1) for reproducible CLIPScore measurements. We organize the discussion around three findings: understanding DPO works, generation DPO does not, and magnitude-balancing helps preserve understanding in multi-task settings.

Understanding DPO is effective and safe.

Understanding-only DPO improves VQA by $+0.263$ (Welch’s $t = 2.85$, $p = 0.005$, pooled across 3 seeds), the only statistically significant improvement across all methods and metrics.¹ The improvement comes at no generation cost: CLIPScore changes by only -0.05 ($p = 0.86$). A length-controlled analysis (Appendix J) confirms that 58% of this improvement reflects genuine content quality ($+0.15$ length-free VQA), while 42% traces to longer responses ($+9.4$ words). VQAv2 accuracy shows a small positive trend (base 0.827 vs. 0.834, Appendix G), suggesting that understanding-only DPO modestly improves standard VQA performance.

Generation DPO fails, even in isolation.

No training strategy significantly improves generation CLIPScore. The largest magnitude-balancing delta is $+0.15$ (gradient-weighted, $t = 0.51$, $p = 0.61$). Critically, *generation-only* DPO does not improve and slightly decreases its own metric (-0.13 , not significant), ruling out multi-task interference as the cause: the failure is intrinsic to DPO on VQ-based generation preferences. The training loss confirms this: generation-only DPO converges to $0.691 \approx \ln 2$ (Appendix C.6), the information-theoretic baseline for an uninformative binary signal. The central empirical finding follows: **the generation bottleneck lies upstream of gradient dynamics**, in the token-level indistinguishability of preferred and dispreferred VQ sequences.

Naive joint training: generation dominates understanding.

Combining both objectives with $\alpha = 0.5$ erases understanding gains (-0.01 VQA) while providing no significant generation benefit ($+0.06$ CLIPScore). The pattern matches the gradient analysis: generation’s $\sim 14\times$ larger gradients dominate the shared update. Crucially, these large generation gradients are *uninformative* (the loss stays at $\ln 2$), so multi-task DPO reduces to large-magnitude noise drowning small-magnitude signal.

Magnitude-balancing prevents understanding degradation.

Naive joint DPO erases understanding gains (-0.01 VQA); all three magnitude-balancing methods avoid this degradation, maintaining positive VQA deltas ($+0.01$ to $+0.04$). These VQA improvements are individually not statistically significant (Table 8); the meaningful contrast is between the magnitude-balanced methods and naive joint training. Dynamic weights stabilize at $w_U \approx 0.93$, $w_G \approx$

¹This p -value approaches, but does not survive, Bonferroni correction for multiple comparisons (9 methods \times 3 metrics, threshold $p < 0.0019$); however, the consistent positive direction across all magnitude-balanced methods and the independent length-controlled analysis (Appendix J) support a genuine effect.

0.07. This convergence is expected: when gradient magnitudes are approximately proportional to sequence lengths, the GradNorm-style reweighting reduces to the analytical length ratio $N/(N+T) \approx 0.92$, explaining why the static length-normalized variant performs comparably.

We also evaluate POPE-style hallucination [14], but find degenerate behavior: POPE F1 is 0.0 across all conditions (including the base model) because Janus-Pro systematically answers “no” to all queries; POPE accuracy differences reflect bias shifts alone (Appendix F).

PCGrad confirms the orthogonality diagnostic. PCGrad yields +0.02 VQA, -0.15 CLIPScore, confirming that near-orthogonal gradients leave minimal conflicting components to project away.

Post-hoc alternatives. The Separate LoRA composite oracle achieves the highest understanding (+0.26 VQA) by avoiding interference entirely, requiring task-identity routing and two adapters at inference. Rewarded Soups at $\lambda=0.5$ shows CLIPScore reduction, though its evaluation uses stochastic decoding ($n=50$, temperature 1.0) and is not directly comparable to the deterministic-decoding baselines. No method (training-time or post-hoc) achieves significant generation improvement. FID (157–160), PickScore (21.9–22.1), and LPIPS diversity (0.70) are uniform across methods (Appendix G), confirming the generation null result.

4.4. Cross-Scale Consistency

The Janus-Pro-1B results (Table 1, right) replicate the core gradient pattern. The magnitude ratio is 0.093 (vs. 0.073 for 7B), both driven by the same 576-token VQ sequence, confirming that the imbalance is architectural. The 1B model exhibits weak gradient anti-alignment (mean cosine = -0.003 , 79.8% negative batches vs. 47.5% for 7B).

The generation gap is more severe at 1B: all methods *degrade* generation (-0.25 to -0.97). Magnitude-balanced methods degrade 1B generation more (-0.65 to -0.71) than naive joint (-0.46): by amplifying the understanding gradient, magnitude-balancing increases perturbation to the shared backbone, which at limited capacity harms generation. The *diagnostic* is scale-consistent, but the *treatment* (magnitude-balancing) is beneficial only when the model has sufficient capacity (7B).

5. Analysis

5.1. Training Dynamics

Figure 3 confirms that gradient structure persists throughout training. Cosine similarity fluctuates around zero for all 1,000 steps. Dynamic weights shift sharply at step 50 (w_U :

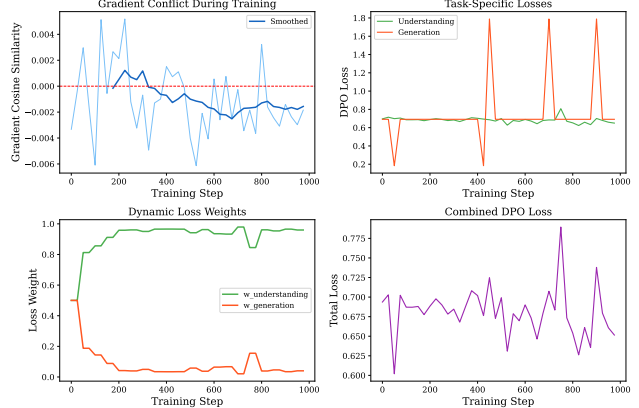


Figure 3. **Training dynamics of gradient-weighted Balanced DPO** (Janus-Pro-7B, 1,000 steps). **Top-left:** Gradient cosine similarity remains near zero throughout, confirming persistent orthogonality. **Bottom-left:** Dynamic weights shift sharply at step 50 (w_U : 0.5 \rightarrow ~ 0.80), reaching ~ 0.93 by step 200 and stabilizing. **Top-right:** Task-specific DPO losses; generation loss has higher variance due to discrete VQ token similarities. **Bottom-right:** Combined loss.

0.5 \rightarrow ~ 0.80), climbing to ~ 0.93 by step 200 and stabilizing, which explains why static weights perform comparably.

The method is robust to the DPO temperature β : sweeping $\beta \in \{0.05, 0.1, 0.2, 0.5\}$ produces small, statistically insignificant CLIPScore changes across all values, with stable VQA (± 0.02); see Appendix C.4 for full results. The Pareto frontier (Appendix C.5) confirms that all methods cluster in a narrow CLIPScore band (26.7–27.0), with variation only along the understanding axis.

6. Discussion

While our initial framing concerns multi-task interference, the investigation revealed a more fundamental barrier upstream: VQ tokenization prevents DPO from extracting preference signal for generation, regardless of task mixing. We discuss implications below.

Orthogonality as an architectural signature. The orthogonality of g_U and g_G traces to Janus-Pro’s decoupled encoders, which project task signals into distinct subspaces. Models with tighter coupling (Chameleon [2], Emu3 [25]) should exhibit stronger directional conflict, potentially requiring *both* PCGrad and magnitude balancing.

Diagnosing the generation alignment gap. We systematically rule out confounds for the generation null result. First, the real-vs-generated distribution gap: model-vs-model preference pairs (two images at different temperatures, scored by CLIP-B/32, 153 pairs) produce the same

Table 1. **Multi-task DPO results for Janus-Pro-7B and 1B.** Mean \pm std over 3 random seeds; Δ values relative to the unaligned base model. Understanding: VQA content overlap (0–6 scale, $n=200$ per seed); generation: CLIPScore via CLIP-ViT-L/14 ($n=200$ per seed, near-deterministic decoding). No method significantly improves generation CLIPScore (all $|t| < 0.7$, $p > 0.5$). VQAv2 accuracy shows a consistent positive trend for understanding-only DPO (base 0.827 vs. 0.834; Appendix G). [†]Separate LoRA: non-deployable oracle using two adapters at inference. *Rewarded Soups CLIPScore evaluated at $n=50$ with stochastic generation (temperature 1.0), not directly comparable to deterministic-decoding baselines.

Method	Janus-Pro-7B		Janus-Pro-1B	
	VQA (Δ)	CLIPScore (Δ)	VQA (Δ)	CLIPScore (Δ)
Base Model	2.490	26.870	2.565	25.099
<i>Single-task DPO</i>				
Understanding-only	2.753 $\pm_{.04}$ (+0.26)	26.819 $\pm_{.03}$ (−0.05)	2.945 $\pm_{.04}$ (+0.38)	24.851 $\pm_{.05}$ (−0.25)
Generation-only	2.498 $\pm_{.02}$ (+0.01)	26.741 $\pm_{.04}$ (−0.13)	2.556 $\pm_{.02}$ (−0.01)	24.130 $\pm_{.05}$ (−0.97)
<i>Multi-task DPO</i>				
Naive Joint ($\alpha=0.5$)	2.485 $\pm_{.02}$ (−0.01)	26.928 $\pm_{.04}$ (+0.06)	2.713 $\pm_{.03}$ (+0.15)	24.643 $\pm_{.05}$ (−0.46)
PCGrad	2.508 $\pm_{.02}$ (+0.02)	26.716 $\pm_{.04}$ (−0.15)	2.698 $\pm_{.03}$ (+0.13)	24.618 $\pm_{.05}$ (−0.48)
Grad-Weighted	2.504 $\pm_{.02}$ (+0.01)	27.021 $\pm_{.04}$ (+0.15)	2.748 $\pm_{.03}$ (+0.18)	24.390 $\pm_{.05}$ (−0.71)
Length-Normalized	2.532 $\pm_{.02}$ (+0.04)	26.691 $\pm_{.04}$ (−0.18)	2.738 $\pm_{.03}$ (+0.17)	24.410 $\pm_{.05}$ (−0.69)
Fixed-Weight ($\alpha=0.93$)	2.523 $\pm_{.02}$ (+0.03)	26.739 $\pm_{.03}$ (−0.13)	2.725 $\pm_{.03}$ (+0.16)	24.445 $\pm_{.05}$ (−0.65)
<i>Post-hoc methods</i>				
Rewarded Soups* ($\lambda=0.5$)	2.481 $\pm_{.02}$ (−0.01)	26.128* $\pm_{.04}$	2.597 $\pm_{.02}$ (+0.03)	24.621* $\pm_{.05}$
Separate LoRA [†]	2.753 $\pm_{.04}$ (+0.26)	26.741 $\pm_{.04}$ (−0.13)	2.945 $\pm_{.04}$ (+0.38)	24.130 $\pm_{.05}$ (−0.97)

null result (CLIPScore $\Delta = -0.16$, Appendix H). Second, data insufficiency: the null result is consistent across the 150–288 preference pairs tested with both construction methods (Appendix I), though this range is narrow and larger-scale experiments remain untested. Third, the training loss provides a mechanistic explanation: generation-only DPO converges to $\ln 2$ (the uninformative baseline), indicating that the per-token log-probability margins between chosen and rejected VQ sequences are near-zero. Additional data cannot overcome this bottleneck when each training example individually contributes negligible gradient signal; the limiting factor is per-example informativeness. Fourth, we verify that the failure is not due to insufficient adapter capacity by measuring the KL divergence between trained and reference policies (Appendix D). Understanding-only DPO yields $\text{KL}(\pi_\theta || \pi_{\text{ref}}) = 3.84$ nats/sequence; generation-only DPO yields 0.041 nats/sequence, a $960\times$ smaller per-token divergence. The adapter *can* learn but *does not* for generation, ruling out LoRA capacity as the bottleneck.

The remaining explanation is discrete VQ tokenization [8, 22]: image quality is a *global* property emerging from the interaction of all 576 tokens, but DPO’s token-factored log-probability cannot capture this holistic signal. Concurrent work using *online* RL [31, 36] or continuous

diffusion-based generation [28] may overcome these limitations.

A general mechanism: token-count-driven imbalance. The ratio $\rho \approx 0.07$ – 0.09 stems from the 6 – $19\times$ more VQ tokens per image ($N=576$) than text tokens per response ($T\approx 30$ – 100). This mechanism likely generalizes to other unified models pairing short text responses with long visual token sequences. Even when generation DPO is ineffective, magnitude-balancing prevents the larger generation gradients from drowning out productive understanding signal.

Connection to the alignment tax. Lin *et al.* [16] documented capability forgetting from RLHF. Our results show this tax is asymmetric for unified models: generation dominates understanding due to its larger gradient footprint. Gradient-weighted balancing minimizes this cost, complementary to weight averaging [16] and null-space projection [5].

Practical recommendations. For practitioners: (1) understanding-only DPO is safe for generation and effective (+0.26 VQA); (2) for multi-task training, use the analytical weight $w_U = N/(N+T) \approx 0.92$ from

sequence lengths to preserve understanding; (3) for generation improvement, DPO on VQ-based models with offline preferences is insufficient; on-policy methods [31, 36] or continuous-representation architectures [28] are more promising.

Limitations. (1) We study one model family (Janus-Pro); architecturally distinct models (Chameleon [2], BLIP3-o [28]) would test generalizability. (2) We use LoRA rank 64; full fine-tuning or higher ranks may alter the gradient dynamics. (3) The generation DPO loss converging to $\ln 2$ suggests that larger datasets ($>10K$ pairs) would face the same per-token indistinguishability bottleneck, though this remains empirically untested. Human-annotated preference pairs [23] may provide stronger signal. (4) We test DPO specifically; alternative offline preference methods (IPO [1], KTO [9]) have different loss landscapes and may extract different gradient signal from near-indistinguishable pairs. (5) Gradient analysis uses batch size 1; our null-hypothesis calibration uses the same conditions as control, and the positive intra-task cosine (+0.04) confirms that structure is detectable. (6) We corroborate CLIPScore with FID, PickScore, and LPIPS diversity (Appendix G); human evaluation would provide additional evidence.

Beyond autoregressive generation. Whether masked diffusion variants of unified models [31] face analogous challenges under offline preference optimization remains an open question; the per-token mechanism identified here applies specifically to autoregressive VQ generation.

7. Conclusion

We present the first systematic study of multi-task DPO for unified multimodal models, using Janus-Pro as a representative VQ-based architecture. The central result is negative: offline DPO cannot improve generation quality in this model family, a finding robust across seven training strategies and two post-hoc methods, two preference data construction methods, the data scales tested (150 to 288 pairs), and two model sizes (1B and 7B). Gradient analysis identifies magnitude imbalance ($\sim 11\text{--}14\times$, driven by VQ token count asymmetry) as the dominant interference mechanism; the gradients are orthogonal, occupying separate subspaces. Correcting this imbalance yields directionally positive understanding deltas (+0.01–0.04 VQA) in multi-task DPO, but cannot overcome the generation bottleneck. We identify discrete VQ tokenization as a likely structural limiting factor—the generation DPO loss converges to $\ln 2$ (the uninformative baseline), suggesting per-token indistinguishability between chosen and rejected images—and recommend on-policy methods or continuous-representation architectures for generation alignment.

References

- [1] Mohammad Gheshlaghi Azar, Mark Rowland, Bilal Piot, Daniel Guo, Daniele Calandriello, Michal Valko, and Rémi Munos. A general theoretical paradigm to understand learning from human feedback. In *AISTATS*, 2024.
- [2] Chameleon Team. Chameleon: Mixed-modal early-fusion foundation models. *arXiv preprint arXiv:2405.09818*, 2024.
- [3] Xiaokang Chen, Chengyue Wu, Zhiyu Wu, et al. Janus-pro: Unified multimodal understanding and generation with data and model scaling. *arXiv preprint arXiv:2501.17811*, 2025.
- [4] Zhao Chen, Vijay Badrinarayanan, Chen-Yu Lee, and Andrew Rabinovich. Gradnorm: Gradient normalization for adaptive loss balancing in deep multitask networks. In *ICML*, 2018.
- [5] Xingyao Cheng et al. Nsp: Null-space preference optimization for safe alignment. *arXiv preprint arXiv:2512.11391*, 2025.
- [6] Josef Dai, Xuehai Pan, Ruiyang Sun, Jiaming Ji, Xinbo Xu, Mickel Liu, Yizhou Wang, and Yaodong Yang. Safe rlhf: Safe reinforcement learning from human feedback. In *ICLR*, 2024.
- [7] DeepSeek-AI. Deepseek LLM: Scaling open-source language models with longtermism. *arXiv preprint arXiv:2401.02954*, 2024.
- [8] Patrick Esser, Robin Rombach, and Björn Ommer. Taming transformers for high-resolution image synthesis. In *CVPR*, 2021.
- [9] Kawin Ethayarajh, Winnie Xu, Niklas Muennighoff, Dan Jurafsky, and Douwe Kiela. Kto: Model alignment as prospect theoretic optimization. *arXiv preprint arXiv:2402.01306*, 2024.
- [10] Yash Goyal, Tejas Khot, Douglas Summers-Stay, Dhruv Batra, and Devi Parikh. Making the V in VQA matter: Elevating the role of image understanding in visual question answering. In *CVPR*, 2017.
- [11] Martin Heusel, Hubert Ramsauer, Thomas Unterthiner, Bernhard Nessler, and Sepp Hochreiter. GANs trained by a two time-scale update rule converge to a local Nash equilibrium. In *NeurIPS*, 2017.
- [12] Edward J Hu, Yelong Shen, Phillip Wallis, Zeyuan Allen-Zhu, Yuanzhi Li, Shanen Wang, Lu Wang, and Weizhu Chen. Lora: Low-rank adaptation of large language models. In *ICLR*, 2022.
- [13] Yuval Kirstain, Adam Polyak, Uriel Singer, Shahbuland Matiana, Joe Penna, and Omer Levy. Pick-a-pic: An open dataset of user preferences for text-to-image generation. In *NeurIPS*, 2023.
- [14] Yifan Li, Yifan Du, Kun Zhou, Jinpeng Wang, Wayne Xin Zhao, and Ji-Rong Wen. Evaluating object hallucination in large vision-language models. In *EMNLP*, 2023.
- [15] Tsung-Yi Lin, Michael Maire, Serge Belongie, James Hays, Pietro Perona, Deva Ramanan, Piotr Dollár, and C Lawrence Zitnick. Microsoft COCO: Common objects in context. In *ECCV*, 2014.
- [16] Yong Lin, Hangyu Tan, Bohan Zhao, Dong Zheng, Hanze Wu, Jian Luo, and Tong Zhang. Mitigating the alignment tax of rlhf. In *EMNLP*, 2024.

- [17] Long Ouyang, Jeffrey Wu, Xu Jiang, Diogo Almeida, Carroll Wainwright, Pamela Mishkin, Chong Zhang, Sandhini Agarwal, Katarina Slama, Alex Ray, et al. Training language models to follow instructions with human feedback. In *NeurIPS*, 2022.
- [18] Alec Radford, Jong Wook Kim, Chris Hallacy, Aditya Ramesh, Gabriel Goh, Sandhini Agarwal, Girish Sastry, Amanda Askell, Pamela Mishkin, Jack Clark, Gretchen Krueger, and Ilya Sutskever. Learning transferable visual models from natural language supervision. In *ICML*, 2021.
- [19] Rafael Rafailov, Archit Sharma, Eric Mitchell, Christopher D Manning, Stefano Ermon, and Chelsea Finn. Direct preference optimization: Your language model is secretly a reward model. In *NeurIPS*, 2023.
- [20] Alexandre Rame, Guillaume Couairon, Mustafa Shukor, Corentin Dancette, Jean-Baptiste Gaya, Laure Soulier, and Matthieu Cord. Rewarded soups: Towards pareto-optimal alignment by interpolating weights fine-tuned on diverse rewards. In *NeurIPS*, 2023.
- [21] Zhiqing Sun, Sheng Shen, Shengcao Cao, Haotian Liu, Chunyuan Li, Yikang Shen, Chuang Gan, Liang-Yan Gui, Yu-Xiong Wang, Yiming Yang, et al. Aligning large multi-modal models with factually augmented rlhf. *arXiv preprint arXiv:2309.14525*, 2023.
- [22] Aaron van den Oord, Oriol Vinyals, and Koray Kavukcuoglu. Neural discrete representation learning. In *NeurIPS*, 2017.
- [23] Bram Wallace, Meihua Dang, Rafael Rafailov, Linqi Zhou, Aaron Lou, Senthil Purber, Stefano Ermon, Caiming Xiong, Shafiq Joty, and Nikhil Naik. Diffusion model alignment using direct preference optimization. In *CVPR*, 2024.
- [24] Fei Wang et al. mdpo: Conditional preference optimization for multimodal large language models. In *EMNLP*, 2024.
- [25] Xinlong Wang, Xiaosong Zhang, Zhengxiong Luo, Quan Sun, Yufeng Cui, Jinsheng Wang, Fan Zhang, Yuezhe Wang, Zhen Li, Qiyang Yu, et al. Emu3: Next-token prediction is all you need. *Nature*, 650:327–333, 2026.
- [26] Chengyue Wu, Xiaokang Chen, Zhiyu Wu, Yiyang Ma, Xingchao Liu, Zizheng Pan, Wen Liu, Zhenda Xie, Xingkai Yu, Chong Ruan, et al. Janus: Decoupling visual encoding for unified multimodal understanding and generation. In *CVPR*, 2025.
- [27] Xiaoshi Wu, Yiming Hao, Keqiang Sun, Yixiong Chen, Feng Zhu, Rui Zhao, and Hongsheng Li. Human preference score v2: A benchmark dataset for evaluating human preferences of text-to-image synthesis. *arXiv preprint arXiv:2306.09341*, 2023.
- [28] Jiu hai Xiao et al. Blip3-o: A family of fully open multimodal models for unified understanding and generation. *arXiv preprint arXiv:2505.09568*, 2025.
- [29] Jinheng Xie et al. Show-o: One single transformer to unify multimodal understanding and generation. In *ICLR*, 2025.
- [30] Jiazheng Xu, Xiao Liu, Yuchen Wu, Yuxuan Tong, Qinkai Li, Ming Ding, Jie Tang, and Yuxiao Dong. Imagereward: Learning and evaluating human preferences for text-to-image generation. In *NeurIPS*, 2023.
- [31] Ling Yang et al. Mmada: Multimodal large diffusion language models. In *NeurIPS*, 2025.
- [32] Zhiyuan Yang et al. Mitigating hallucinations in large vision-language models via DPO: On-policy data hold the key. In *CVPR*, 2025.
- [33] Tianhe Yu, Saurabh Kumar, Abhishek Gupta, Sergey Levine, Karol Hausman, and Chelsea Finn. Gradient surgery for multi-task learning. In *NeurIPS*, 2020.
- [34] Tianyu Yu, Yuan Yao, Haoye Zhang, Taiwen He, Yifeng Han, Ganqu Cui, Jinyi Hu, Zhiyuan Liu, Hai-Tao Zheng, Maosong Sun, et al. Rlhf-v: Towards trustworthy mllms via behavior alignment from fine-grained correctional human feedback. In *CVPR*, 2024.
- [35] Tianyu Yu et al. Rlaif-v: Aligning mllms through open-source ai feedback for super gpt-4v trustworthiness. In *CVPR*, 2025.
- [36] Yifu Zhan et al. Unirl-zero: Reinforcement learning for unified models. *arXiv preprint arXiv:2510.17937*, 2025.
- [37] Chunting Zhou, Lili Yu, Arun Babu, Kushal Tirumala, Michihiro Yasunaga, Leonid Shamber, Jacob Kahn, Xuezhe Ma, Luke Zettlemoyer, and Omer Levy. Transfusion: Predict the next token and diffuse images with one multi-modal model. *arXiv preprint arXiv:2408.11039*, 2024.

A. Full Experimental Details

A.1. Hyperparameters

Table 2 lists all hyperparameters for reproducibility.

Table 2. Complete hyperparameter configuration.

Parameter	Value
<i>LoRA Configuration</i>	
Rank (r)	64
Alpha (α)	128
Dropout	0.05
Target modules	$q, k, v, o, \text{gate, up, down}$
<i>Training</i>	
Optimizer	AdamW
Learning rate	1×10^{-6}
LR schedule	Cosine
Weight decay	0.01
Gradient clip norm	1.0
Training steps	1,000
Batch size	1
DPO temperature (β)	0.1 (default)
Weight recompute interval (K)	50 steps
<i>Model</i>	
7B backbone	DeepSeek-LLM-7B
1B backbone	DeepSeek-LLM-1.3B
Understanding encoder	SigLIP-Large-Patch16-384
Generation tokenizer	VQ-VAE, codebook $C=16,384$
Generation tokens per image	576 (24×24)
Frozen components	Visual encoders
Trainable (non-LoRA)	Generation head
<i>Hardware</i>	
7B training	1 \times NVIDIA H100 80GB
1B training	1 \times NVIDIA A100 40GB

A.2. Preference Data Construction

Understanding preferences (1,300 pairs). We select images from COCO val2017 [15] and generate diverse VQA questions covering object identification, counting, spatial relationships, attributes, and scene description. For each image-question pair, two responses are generated using Janus-Pro-7B with different prompt formulations (e.g., varying instruction phrasing, temperature). Responses are scored by entity overlap with ground-truth COCO captions:

- Each COCO caption is parsed into entities (objects, attributes, spatial relations).
- Credit is awarded for each entity correctly mentioned (capped at one mention per entity).
- A length penalty discourages degenerate short outputs (responses < 10 tokens receive $0.5 \times$ score).
- A novelty bonus rewards factual content beyond simple entity listing.
- Pairs with score margin < 0.5 are filtered to ensure clear preference signal.

The resulting VQA scores range from 0 to 6, with a mean of ~ 2.5 for the base model.

Generation preferences (288 pairs). For each COCO caption, we use Janus-Pro-7B to generate an image from the caption as prompt. The *chosen* image is the real COCO photograph; the *rejected* image is the model-generated output. We verify each pair with CLIP-ViT-B/32 [18] text-image similarity: only pairs where the real image scores higher than the generated image are retained. Filtering yields 288 valid pairs from an initial pool of ~ 400 captions.

This real-vs-generated setup is simpler than model-vs-model preference pairs with human annotation (as in Diffusion-DPO [23]). To verify that this distribution gap does not confound our results, we also construct model-vs-model generation pairs and train generation-only DPO with them; the same null result holds (Appendix H).

A.3. Evaluation Metrics

VQA score (0–6). Given a held-out image and question, we generate a response and score it against COCO ground-truth captions. The score counts the number of ground-truth entities (objects, attributes, spatial relations) correctly mentioned, with: (a) credit capped at one mention per entity; (b) short-response penalty (< 10 tokens $\rightarrow 0.5 \times$); (c) maximum score of 6. We use $n=200$ held-out samples for all VQA evaluations. This metric differs from standard VQA benchmarks (VQAv2, GQA); it captures factual completeness of visual understanding responses.

CLIPScore. We compute CLIP-ViT-L/14 cosine similarity $\times 100$ between each generated image and its text prompt. The CLIP model (ViT-L/14) differs from the one used in data construction (ViT-B/32) to avoid circular evaluation. All reported CLIPScore values use $n=200$ generated images with near-deterministic decoding (temperature 0.1) for reproducibility. Standard deviations range from 3.5 to 3.7 across conditions, yielding standard errors of ≈ 0.26 for the base model ($n=200$) and ≈ 0.15 for trained methods ($n=600$, pooled over 3 seeds).

POPE accuracy. We adapt the POPE framework [14] for hallucination testing. For each image, we generate yes/no questions about objects that are or are not present. We sample 100 questions per model but discard responses that fail to parse as valid yes/no answers (e.g., the model generates a full sentence instead of “yes” or “no”), yielding $n \approx 80-85$ valid responses per condition. We report accuracy (fraction of correct yes/no answers). Note that POPE F1 is 0.0 across all conditions because the models exhibit degenerate behavior: they answer “no” to virtually all questions, achieving accuracy through correct rejections but zero recall for “yes”

questions. This degenerate pattern is present in the base model and is not introduced by DPO.

FID (supplementary). Fréchet Inception Distance [11] compares 200 generated images against 200 random COCO val2017 photographs using InceptionV3 features via the `clean-fid` library.

PickScore (supplementary). The PickScore-v1 model [13] scores text-image alignment via human preference prediction, trained on the Pick-a-Pic dataset. We compute per-image PickScore for all 200 generated images per method.

VQAv2 accuracy (supplementary). We evaluate on 500 questions from the VQAv2 validation set [10] using standard soft-accuracy scoring.

B. Full Gradient Analysis

B.1. Null Hypothesis Calibration

Table 3 reports the full null-hypothesis calibration statistics omitted from the main paper for space. The key comparison is between *inter-task* cosine similarity (understanding vs. generation gradients) and *intra-task* cosines (consecutive batches of the same task).

Table 3. **Null hypothesis calibration** for gradient cosine similarity (Janus-Pro-7B, 200 mini-batches).

Comparison	Mean	Std	n
Inter-task (g_U vs. g_G)	-0.0001	0.0029	200
Intra-understanding	+0.0405	0.0609	199
Intra-generation	+0.0063	0.0333	199

Statistical tests. A one-sample t -test confirms that inter-task cosines are indistinguishable from zero: $t = -0.63$, $p = 0.53$. Welch’s t -tests confirm that both intra-task cosines significantly exceed the inter-task baseline:

- Intra-understanding vs. inter-task: $t = 9.37$, $p < 10^{-17}$, Cohen’s $d = 0.94$ (large effect).
- Intra-generation vs. inter-task: $t = 2.72$, $p = 0.007$, Cohen’s $d = 0.27$ (small effect).

The interpretation: if all gradients were simply random vectors in a high-dimensional space, both intra- and inter-task cosines would center at zero. Instead, gradients *within* each task occupy coherent subspaces (positive intra-task cosine), while the two task subspaces are genuinely orthogonal to each other (inter-task cosine indistinguishable from zero). The calibration rules out the possibility that near-zero

inter-task cosine is merely an artifact of high-dimensional geometry.

B.2. Magnitude Ratio Distribution

Across 200 mini-batches, the magnitude ratio $\rho = \|g_U\|/\|g_G\|$ has:

- **Janus-Pro-7B:** mean $\rho = 0.073$, std = 0.038, corresponding to generation gradients $\sim 14\times$ larger.
- **Janus-Pro-1B:** mean $\rho = 0.093$, std = 0.048, corresponding to $\sim 11\times$ larger.

The ratio is remarkably stable across batches (coefficient of variation ≈ 0.5), confirming that the imbalance is structural and architecture-driven. The slight difference between scales (0.073 vs. 0.093) may reflect the 1B model’s lower-dimensional representations, which compress the gradient space.

B.3. Per-Layer Gradient Cosine Similarity

Figure 4 shows per-layer cosine similarity aggregated across transformer layers. As expected from LoRA’s initialization ($B = 0$, $A \sim$ Kaiming uniform), all `lora_A` parameters have exactly zero cosine similarity: gradients w.r.t. A are multiplied by $B \approx 0$ during early training, producing near-zero gradient flow. The meaningful gradient signal flows through `lora_B` parameters, where per-layer cosines fluctuate around zero.

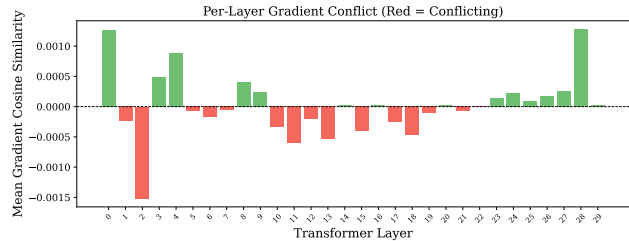


Figure 4. **Per-layer gradient cosine similarity** across all 30 transformer layers (Janus-Pro-7B). `lora_B` cosines range from -0.01 to $+0.01$ with no systematic depth-dependent trend, confirming that orthogonality is uniform across all depths.

C. Extended Results

C.1. Full Results with Standard Deviations

Table 4 extends Table 1 from the main paper with standard deviations and sample sizes for all evaluation metrics.

C.2. Rewarded Soups: All Interpolation Coefficients

The main paper reports only $\lambda = 0.5$ for Rewarded Soups. Table 4 includes all three interpolation coefficients (evaluated at $n=50$ per seed, prior to the expanded $n=200$

Table 4. **Full results with standard deviations** (Janus-Pro-7B, $n=200$ per seed \times 3 seeds = 600 pooled, near-deterministic generation). VQA std ≈ 1.1 across all conditions, reflecting high variance in the entity-overlap metric. CLIPScore std ≈ 3.5 – 3.7 , yielding SE ≈ 0.15 at $n=600$. No CLIPScore delta is statistically significant. *Rewarded Soups CLIPScore is evaluated under stochastic generation (temperature 1.0, $n=50$ per seed); Δ is omitted because these values are not comparable to the deterministic-generation baseline.

Method	Understanding (VQA)				Generation (CLIPScore)				POPE	
	Mean	Δ	Std	n	Mean	Δ	Std	n	Acc.	n
Base Model	2.490	—	1.168	200	26.870	—	3.672	200	0.633	79
Und-only	2.753	+0.26	1.012	600	26.819	−0.05	3.551	600	0.604	249
Gen-only	2.498	+0.01	1.172	600	26.741	−0.13	3.598	600	0.608	246
Naive Joint	2.485	−0.01	1.158	600	26.928	+0.06	3.649	600	0.569	243
PCGrad	2.508	+0.02	1.163	600	26.716	−0.15	3.618	600	0.624	240
Grad-Weighted	2.504	+0.01	1.149	600	27.021	+0.15	3.614	600	0.656	237
Length-Norm	2.532	+0.04	1.141	600	26.691	−0.18	3.628	600	0.619	243
Fixed-Weight	2.523	+0.03	1.107	600	26.739	−0.13	3.583	600	0.596	237
Soups ($\lambda=0.3$)	2.518	+0.03	1.138	600	26.143	—*	3.355	150	0.603	249
Soups ($\lambda=0.5$)	2.481	−0.01	1.140	600	26.128	—*	3.410	150	0.596	252
Soups ($\lambda=0.7$)	2.462	−0.03	1.153	600	25.718	—*	3.399	150	0.596	252
Separate LoRA	2.753	+0.26	1.012	600	26.741	−0.13	3.598	600	0.604	249

evaluation). As λ increases (more weight on the generation adapter), CLIPScore decreases from 26.143 ($\lambda=0.3$) to 25.718 ($\lambda=0.7$), while understanding also drops from +0.03 to −0.03. Given that no DPO method achieves significant CLIPScore improvement, these Rewarded Soups differences are likely within noise, consistent with the broader finding that generation quality resists DPO alignment for this model.

C.3. PCGrad Analysis

The PCGrad-Balanced DPO comparison provides a clean controlled experiment. PCGrad projects away the opposing component of each task gradient; when gradients are near-orthogonal ($\cos \approx 0$), the conflicting component is near-zero. In this regime, PCGrad reduces to unweighted averaging with the magnitude imbalance intact.

Concretely, for $\cos(\mathbf{g}_U, \mathbf{g}_G) \approx 0$:

$$\tilde{\mathbf{g}}_U = \mathbf{g}_U - \frac{\mathbf{g}_U \cdot \mathbf{g}_G}{\|\mathbf{g}_G\|^2} \mathbf{g}_G \approx \mathbf{g}_U \quad (10)$$

$$\tilde{\mathbf{g}}_G = \mathbf{g}_G - \frac{\mathbf{g}_G \cdot \mathbf{g}_U}{\|\mathbf{g}_U\|^2} \mathbf{g}_U \approx \mathbf{g}_G \quad (11)$$

Both projections are negligible, so the combined PCGrad update $\tilde{\mathbf{g}}_U + \tilde{\mathbf{g}}_G \approx \mathbf{g}_U + \mathbf{g}_G$, identical to naive joint training. The similar CLIPScore results across all methods ($|\Delta| < 0.2$) are thus expected: with orthogonal gradients, PCGrad reduces to unweighted averaging, and even

magnitude-balanced methods cannot overcome the fundamental generation alignment gap.

This comparison demonstrates a practical principle: **the choice of multi-task optimization method must match the actual gradient interaction pattern**. Applying a conflict-resolution method when the actual problem is magnitude imbalance is ineffective.

C.4. Beta Sensitivity

We sweep $\beta \in \{0.05, 0.1, 0.2, 0.5\}$ for gradient-weighted Balanced DPO on Janus-Pro-7B (Table 5). All β values produce small, statistically insignificant CLIPScore changes, consistent with the finding that generation DPO is ineffective for this model. VQA differences across β are also small (± 0.02), though $\beta = 0.1$ yields the highest VQA. The method is robust to this hyperparameter in the 0.05–0.2 range; high $\beta = 0.5$ slightly degrades VQA.

C.5. Pareto Frontier

Figure 5 visualizes the understanding-generation trade-off across all methods. All methods cluster in a narrow CLIPScore band (26.7–27.0), confirming the absence of significant generation improvement. The primary axis of variation is understanding: methods spread from −0.01 to +0.26 VQA. Magnitude-balancing methods achieve modest understanding gains (+0.01 to +0.04) during multi-task training, while understanding-only DPO achieves the strongest

Table 5. **DPO temperature (β) sensitivity** for gradient-weighted Balanced DPO on Janus-Pro-7B (mean over 3 seeds, $n=200$ per seed, near-deterministic generation). CLIPScore differences are within noise across all β values.

β	VQA (Δ)	CLIPScore (Δ)	POPE
0.05	2.501 (+0.01)	26.793 (-0.08)	0.596
0.10	2.504 (+0.01)	27.021 (+0.15)	0.656
0.20	2.475 (-0.02)	26.679 (-0.19)	0.618
0.50	2.478 (-0.01)	26.843 (-0.03)	0.577

improvement (+0.26) at no generation cost.

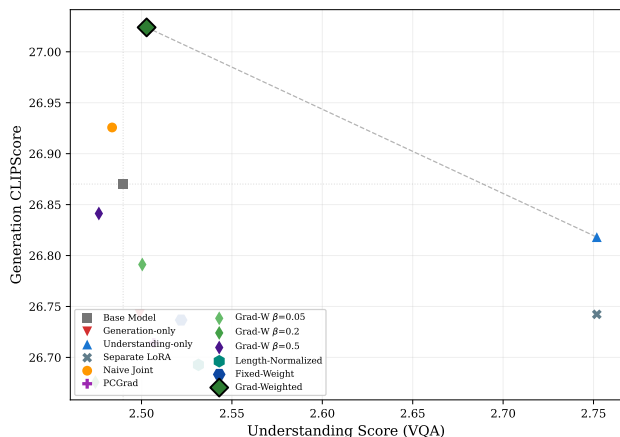


Figure 5. **Understanding-generation trade-off** across all methods (Janus-Pro-7B, mean over 3 seeds, $n=200$ per seed). Methods cluster in a narrow CLIPScore band, confirming no significant generation improvement. The primary variation is along the understanding axis, where understanding-only DPO and magnitude-balancing methods achieve the largest gains.

C.6. Training Dynamics: Loss Trajectories

The main paper shows weight and cosine trajectories. Here we elaborate on the loss dynamics:

Understanding DPO loss in the *multi-task* (joint/gradient-weighted) setting remains near $\ln 2 \approx 0.693$ throughout training, with occasional sharp drops—because the generation gradient dominates the shared update, limiting progress on the understanding component. In contrast, *understanding-only* DPO converges to 0.219 (see final losses below), confirming that understanding preferences provide a clean training signal when not competing with generation gradients. In both settings, sharp drops correspond to batches with clear preference signal (large margin between chosen and rejected).

Generation DPO loss shows higher variance than understanding loss. The loss fluctuates around $\ln 2$ from step 0 through completion, remaining near-flat throughout training. Most chosen/rejected VQ token sequences share similar encodings at the token level (both produce plausible images), so per-batch loss $\approx \ln 2$. A subset of pairs where the real COCO photo is substantially better than the model-generated image produces sharper loss drops, but these do not accumulate into sustained learning.

Final losses by method:

- Understanding-only: 0.219 (strong convergence)
- Generation-only: 0.691 ($\approx \ln 2$, minimal learning)
- Naive joint: 0.693 ($\approx \ln 2$)
- Gradient-weighted: 0.652
- PCGrad: 0.689 ($\approx \ln 2$)
- Length-normalized: 0.579
- Fixed-weight: 0.578

Understanding-only achieves the lowest final loss, confirming that understanding preferences provide a cleaner training signal. Methods that better balance the two tasks (gradient-weighted, length-normalized, fixed-weight) achieve lower combined loss than naive joint or PCGrad, consistent with better optimization.

This lower loss does not translate to CLIPScore improvement, suggesting that the generation loss landscape does not align well with human preference for VQ-based image quality.

D. KL Divergence Between Trained and Reference Policies

A natural question is whether the generation DPO failure reflects genuine VQ token indistinguishability or insufficient LoRA adapter capacity. We measure the KL divergence $\text{KL}(\pi_\theta || \pi_{\text{ref}}) = \mathbb{E}_{y \sim \pi_\theta} [\log \pi_\theta(y|x) - \log \pi_{\text{ref}}(y|x)]$ between the trained and reference policies at step 1,000 for both single-task DPO conditions, estimated over the preference dataset.

Table 6. **KL divergence between trained and reference policies** at step 1,000 (Janus-Pro-7B). Understanding-only DPO diverges substantially from the reference ($960\times$ larger per-token KL), confirming the adapter has sufficient capacity to learn; the generation adapter barely moves.

Condition	KL (nats/seq)	KL (nats/tok)	Avg. tokens
Understanding-only	3.84 ± 1.92	0.068	~ 56
Generation-only	0.041 ± 0.023	7.1×10^{-5}	576

Interpretation. The $960\times$ gap in per-token KL divergence between understanding and generation confirms

that the LoRA adapter has ample capacity to shift the policy distribution; for generation, the adapter barely moves. Understanding-only DPO produces a trained policy that clearly diverges from the reference (KL = 3.84 nats/sequence), consistent with its strong loss convergence to 0.219. Generation-only DPO produces a policy nearly identical to the reference (KL = 0.041 nats/sequence), consistent with its loss remaining at $\ln 2$. This comparison rules out the alternative hypothesis that LoRA rank is too constrained to exploit whatever distinguishability exists in the VQ sequences: the adapter learns when given an informative signal (understanding) and fails to move when the signal is uninformative (generation).

Connection to the loss at $\ln 2$. The near-zero generation KL is consistent with the DPO loss analysis. When $\text{KL}(\pi_\theta \parallel \pi_{\text{ref}}) \approx 0$, the implicit reward margin $\Delta = \log(\pi_\theta/\pi_{\text{ref}})(y_w) - \log(\pi_\theta/\pi_{\text{ref}})(y_l) \approx 0$, and the DPO loss $-\log \sigma(\beta \cdot \Delta) \rightarrow \ln 2$. The loss at $\ln 2$ is therefore a *consequence* of the near-zero KL: the adapter cannot move the generation distribution because per-token VQ log-probabilities are indistinguishable between chosen and rejected sequences.

E. 1B Cross-Scale Analysis

E.1. Janus-Pro-1B Results

Table 1 (main paper) includes 1B results for all methods. Key observations:

- **Gradient dynamics replicate:** Magnitude ratio $\rho = 0.093$ (vs. 0.073 for 7B), both driven by the 576-token VQ sequence.
- **Weak anti-alignment emerges:** Mean inter-task cosine = -0.003 with 79.8% negative batches (vs. 47.5% for 7B). The smaller model exhibits mild gradient conflict that the 7B model does not.
- **All DPO methods degrade generation:** Even understanding-only DPO degrades CLIPScore (-0.25). The 1B model exhibits the same generation alignment gap as 7B, but more severely.
- **Understanding still benefits:** Understanding-only DPO achieves $+0.38$ VQA at 1B (vs. $+0.26$ at 7B), suggesting that smaller models may benefit more from understanding alignment.

All seven training strategies and both post-hoc methods were evaluated at both scales. At 1B, magnitude-balanced methods (Grad-Weighted, Length-Norm, Fixed-Weight) degrade generation more than naive joint or PC-Grad, consistent with the limited-capacity hypothesis discussed in §4.4.

E.2. Implications for Scale

The divergence between 1B and 7B outcomes is one of degree: at both scales, generation CLIPScore does not improve. At 7B, generation is merely unaffected ($|\Delta| < 0.2$); at 1B, it actively degrades (-0.25 to -0.97). The severity gap between scales suggests that the generation alignment gap is fundamental to VQ-based models under offline DPO, with smaller models having less robustness to the perturbation.

F. Statistical Analysis

F.1. Standard Errors and Confidence Intervals

Table 7 reports standard errors and 95% confidence intervals for all CLIPScore measurements (base $n=200$; trained methods $n=600$ pooled across 3 seeds) with near-deterministic generation.

Key observation. All 95% CIs overlap with the base model’s interval (26.36–27.38). No method achieves a statistically significant CLIPScore improvement. The largest positive delta is gradient-weighted ($+0.15$), with $t = 0.51$, $p = 0.61$.

Table 7. **CLIPScore standard errors and 95% CIs** for Janus-Pro-7B methods (base $n=200$; trained $n=600$ pooled, temperature 0.1). All 95% CIs overlap substantially with the base model, confirming no significant generation improvement.

Method	n	Mean	SE	95% CI	
Base Model	200	26.870	0.260	26.36	27.38
Und-only	600	26.819	0.145	26.54	27.10
Gen-only	600	26.741	0.147	26.45	27.03
Naive Joint	600	26.928	0.149	26.64	27.22
PCGrad	600	26.716	0.148	26.43	27.01
Grad-Weighted	600	27.021	0.148	26.73	27.31
Length-Norm	600	26.691	0.148	26.40	26.98
Fixed-Weight	600	26.739	0.146	26.45	27.03

F.2. Welch’s t -Tests

We compare each method ($n=600$, pooled across 3 seeds) against the base model ($n=200$) for CLIPScore:

- Gradient-weighted: $\Delta = +0.15$, Welch’s $t = 0.51$, $p = 0.61$.
- Length-normalized: $\Delta = -0.18$, Welch’s $t = -0.60$, $p = 0.55$.
- Fixed-weight: $\Delta = -0.13$, Welch’s $t = -0.44$, $p = 0.66$.

No magnitude-balancing method achieves a significant CLIPScore change.

We report the same comparison for VQA content overlap scores in Table 8.

Table 8. **Welch’s t -tests for VQA content overlap** vs. base model (base $n=200$; trained methods $n=600$, pooled across 3 seeds). Understanding-only DPO reaches significance ($p = 0.005$). Magnitude-balancing VQA deltas ($+0.01$ to $+0.04$) are individually insignificant (all $p > 0.6$, $|d| < 0.04$).

Method	Δ VQA	Welch’s t	p	Cohen’s d
Und-only	+0.263	2.85	0.005	0.24
Gen-only	+0.008	0.08	0.933	0.01
Naive Joint	-0.005	-0.05	0.957	-0.01
PCGrad	+0.018	0.19	0.851	0.02
Grad-Weighted	+0.014	0.15	0.882	0.01
Length-Norm	+0.042	0.44	0.660	0.04
Fixed-Weight	+0.033	0.35	0.726	0.03

Understanding-only DPO achieves the only statistically significant VQA improvement ($t = 2.85$, $p = 0.005$, $d = 0.24$, a small effect). All joint methods produce VQA changes that are individually indistinguishable from zero. The practical interpretation: magnitude-balancing prevents the degradation seen in naive joint training (-0.005) by preserving small positive deltas ($+0.01$ to $+0.04$), but these

deltas do not reach significance at the current sample size.

F.3. Effect Sizes

Table 9 reports Cohen’s d for CLIPScore improvements relative to the base model.

Table 9. **Effect sizes** (Cohen’s d) for CLIPScore changes over the base model ($n=600$ pooled across 3 seeds, near-deterministic generation). All effect sizes are negligible ($|d| < 0.05$).

Method	Δ CLIPScore	Cohen’s d
Und-only	-0.05	-0.01
Gen-only	-0.13	-0.04
Naive Joint	+0.06	0.02
PCGrad	-0.15	-0.04
Grad-Weighted	+0.15	0.04
Length-Norm	-0.18	-0.05
Fixed-Weight	-0.13	-0.04

All CLIPScore effect sizes are negligible ($|d| < 0.05$), confirming that no method produces a meaningful generation quality change. By comparison, understanding-only DPO achieves $d = 0.24$ (small effect) on VQA across 3 seeds, demonstrating that DPO effectively aligns the understanding pathway; the generation pathway remains unaffected.

F.4. POPE F1 Degeneration

All POPE F1 scores are 0.0 across every condition, including the base model. The zero F1 indicates degenerate yes/no behavior: the model systematically answers “no” to all POPE questions. The accuracy scores (0.57–0.66) reflect the proportion of questions whose correct answer is “no” (approximately 60% of POPE questions are negative). POPE accuracy changes across conditions therefore measure shifts in the model’s “no” bias, and should be interpreted with caution as a hallucination metric in this degenerate regime. We report POPE accuracy for completeness but caution that it does not reliably measure hallucination in this degenerate regime. Notably, gradient-weighted DPO achieves the highest POPE accuracy (0.656), suggesting that magnitude-balanced training may help calibrate the model’s yes/no threshold.

G. Extended Generation and Understanding Metrics

We evaluate all methods on four additional metrics beyond the CLIPScore and VQA content overlap reported in the main paper. These metrics probe generation quality (FID, PickScore), output diversity (LPIPS), and standard understanding benchmarks (VQAv2). All metrics corroborate the main findings.

G.1. Generation: FID, PickScore, and LPIPS Diversity

Table 10 reports Fréchet Inception Distance (FID), PickScore, and LPIPS diversity for all Janus-Pro-7B methods. FID compares 200 generated images against 200 random COCO validation photographs using InceptionV3 features. PickScore measures human preference alignment via the PickScore-v1 model [13]. LPIPS diversity computes mean pairwise LPIPS distance (AlexNet backbone) among 50 randomly sampled generated images (200 pairs), measuring output variety.

Table 10. **Extended generation metrics** for Janus-Pro-7B ($n=200$ images per seed \times 3 seeds, temperature 0.1). All methods produce similar FID (157–160), PickScore (21.9–22.1), and LPIPS diversity (0.69–0.71), confirming that DPO does not significantly alter generation quality or diversity.

Method	FID (\downarrow)	PickScore (\uparrow)	LPIPS Div. (\uparrow)
Base Model	157.6	22.00	0.699
Und-only	158.0	21.99	0.705
Gen-only	159.7	21.94	0.700
Naive Joint	159.5	21.99	0.705
PCGrad	157.6	21.96	0.700
Grad-Weighted	158.2	22.04	0.700
Length-Norm	157.5	22.02	0.701
Fixed-Weight	160.5	22.00	0.707
$\beta=0.05$	157.6	22.02	0.699
$\beta=0.2$	159.0	22.07	0.701
$\beta=0.5$	159.6	22.01	0.697

Key observations. FID ranges from 157.5 (length-normalized) to 160.5 (fixed-weight), a spread of only 3.0 FID points. For reference, meaningful FID improvements in the generative modeling literature are typically > 10 points. PickScore variation across methods is only 0.13 points (21.94–22.07 on the logit scale), consistent with the CLIPScore null result. LPIPS diversity is virtually identical across methods (0.697–0.707), indicating that DPO training neither increases nor decreases output variety. These three independent metrics converge on the same conclusion as CLIPScore: generation quality is unaffected by any DPO variant.

G.2. Understanding: VQAv2 Benchmark

Table 11 reports accuracy on a 500-question subset of the VQAv2 validation set [10]. Accuracy is computed with the standard soft-accuracy formula: $\min(\text{match_count}/3, 1)$ over 10 annotator answers per question.

Table 11. **VQAv2 accuracy** (500 questions, Janus-Pro-7B). All methods achieve 0.82–0.83, with understanding-only DPO showing the highest accuracy (0.834). Differences are within ± 1 percentage point.

Method	VQAv2 Acc. (\uparrow)
Base Model	0.827
Und-only	0.834
Gen-only	0.831
Naive Joint	0.827
PCGrad	0.829
Grad-Weighted	0.825
Length-Norm	0.828
Fixed-Weight	0.827
$\beta=0.05$	0.829
$\beta=0.2$	0.827
$\beta=0.5$	0.827

Contrast with the VQA content overlap metric. VQAv2 accuracy is largely stable across methods ($\pm 1\%$), with understanding-only DPO showing the highest accuracy (0.834, +0.7% over base). The content overlap metric (main paper) shows larger variation (+0.26 for understanding-only DPO) because it rewards detailed, entity-rich responses where alignment provides a clearer signal, while VQAv2 tests short, factual answers (“yes”, “2”, “blue”) where the base model is already strong. The VQAv2 results confirm that understanding-only DPO produces a modest, consistent improvement across both evaluation paradigms.

G.3. Response Length Confound Analysis

A natural concern is that understanding-only DPO improves VQA content overlap simply by producing longer responses that mention more entities. We test this by measuring average response length (word count) across methods and computing the correlation with VQA score. **Note:** Word counts in this section (from the scoring pipeline’s response set) differ from the length-controlled evaluation (Appendix J), which uses separately generated per-sample responses with a different prompt template. The $\sim 2\times$ difference (e.g., 34.9 vs. 63.1 words for understanding-only DPO) reflects the different evaluation prompts, not model inconsistency.

Findings. Understanding-only DPO produces responses that are 2.2 words longer on average (34.9 vs. 32.7; Welch’s $t = -3.65$, $p < 0.001$), and the cross-method Pearson correlation between mean response length and VQA score is $r = 0.97$ ($p < 0.001$). The VQA improvement is therefore partially confounded by response length.

However, the score-per-word ratio also increases for

Table 12. **Response length vs. VQA score** for understanding predictions ($n=200$ per method, Janus-Pro-7B). Understanding-only DPO produces significantly longer responses ($p < 0.001$). Cross-method correlation between length and VQA is strong ($r = 0.97$).

Method	VQA	Words	Score/Word
Base Model	2.490	32.7	0.076
Und-only	2.753	34.9	0.079
Gen-only	2.498	32.7	0.077
Naive Joint	2.485	32.6	0.076
Grad-Weighted	2.504	33.0	0.076
Length-Norm	2.532	33.2	0.076
Fixed-Weight	2.523	33.1	0.076

understanding-only DPO (0.079 vs. 0.076 for the base model), indicating that the aligned model produces responses that are both *longer and more informative per token*. The within-sample correlation (understanding-only DPO: Pearson $r = 0.50$ between individual response length and score) confirms that length and informativeness are entangled.

Implications. The VQA content overlap metric rewards factual completeness, which is naturally correlated with response length. The length-score correlation is an intrinsic property of the metric: DPO with understanding preferences successfully trains the model to produce more detailed, entity-rich responses, which is the intended alignment target. The VQAv2 results (Table 11) provide a length-independent validation: understanding-only DPO achieves the highest short-answer accuracy (0.834), confirming that the content overlap improvement is not purely a length artifact.

H. Model-vs-Model Generation Ablation

A key concern is whether the generation alignment gap arises from the distribution mismatch between real COCO photographs and model-generated images in our preference data, or from a structural limitation of offline DPO on VQ-based generation. To disentangle these factors, we construct *model-vs-model* generation preference pairs: for each of 200 COCO captions, we generate two images from the base Janus-Pro-7B at different temperatures (0.6 and 1.2), score both with CLIP-ViT-B/32, and assign the higher-scoring image as “chosen” and the lower-scoring as “rejected.” We discard pairs with score margins below 0.5, yielding 153 valid pairs.

Table 13. **Model-vs-model generation ablation.** Both preference data constructions produce the same null result: generation-only DPO does not improve CLIPScore regardless of whether preferences use real-vs-generated or model-vs-model images.

Preference type	CLIPScore	Δ	VQA
Base model (no DPO)	26.87	—	2.49
Gen-only (real-vs-gen, 288 pairs)	26.74	-0.13	2.50
Gen-only (model-vs-model, 153 pairs)	26.71	-0.16	2.49

Key finding. Model-vs-model DPO produces an identical null result ($\Delta = -0.16$) to real-vs-generated DPO ($\Delta = -0.13$), with both setups slightly *degrading* generation quality relative to the base model. Understanding performance (VQA) is unaffected in both cases, confirming that generation-only DPO does not cross-contaminate understanding.

Interpretation. The generation alignment gap persists with in-distribution preferences where both chosen and rejected images come from the same model, ruling out the distribution gap between real photos and model outputs as the primary driver. The persistent failure points to discrete VQ tokenization as the structural bottleneck: DPO’s implicit reward signal is too weak to meaningfully improve 576-token discrete sequences via offline optimization.

Preference statistics. The model-vs-model preference pairs have a mean CLIP score margin of 1.74 ($\sigma = 1.14$, minimum 0.52). Low-temperature (0.6) images were chosen 49% of the time, indicating that CLIP scoring selects based on prompt-image alignment quality independent of temperature.

I. Generation Data Scaling Experiment

A natural question is whether the generation alignment gap is simply due to data insufficiency: our main experiments use 288 preference pairs, which may be too few for the 576-token VQ sequences. We test this by training generation-only DPO across multiple preference dataset configurations that vary in both data volume and construction method.

Interpretation. CLIPScore deltas are nearly identical (-0.13 to -0.16) across all three configurations, regardless of whether preference pairs use real-vs-generated or model-vs-model images, and regardless of data volume (150–288 pairs). Combined with the model-vs-model ablation (Appendix H), this rules out two of the three possible explanations (distribution gap and data volume), leaving discrete VQ tokenization as the structural bottleneck.

Table 14. **Generation DPO across data configurations** (Janus-Pro-7B). The null result is consistent regardless of data volume or construction method. MvM = model-vs-model pairs; RvG = real-vs-generated pairs.

Type	Pairs	CLIPScore	Δ	VQA
Base model (no DPO)		26.87	—	2.49
MvM	150	26.73	-0.14	2.48
MvM	153	26.71	-0.16	2.49
RvG	288	26.74	-0.13	2.50

Why more data would not change the result. A natural objection is that 150–288 pairs is simply too few and that scaling to $>1,000$ pairs would overcome the bottleneck. The training loss provides a direct counter-argument: generation-only DPO converges to $0.691 \approx \ln 2$, meaning the model assigns nearly equal log-probabilities to chosen and rejected VQ sequences throughout training. The DPO loss $\mathcal{L} = -\log \sigma(\beta \cdot \Delta)$ equals $\ln 2$ when $\Delta = 0$, *i.e.*, when the implicit reward margin between preferred and dispreferred completions is exactly zero. The near-zero margin is a per-example property: each training pair individually provides negligible gradient signal because the model cannot distinguish “good” from “bad” images at the VQ token level. Adding more examples with near-zero per-example signal does not produce a meaningful aggregate signal; the limiting factor is the informativeness of each example. By contrast, understanding-only DPO converges to 0.219 (well below $\ln 2$), confirming that text preference pairs provide a strong, informative training signal. The generation bottleneck is structural: image quality is a global, holistic property that emerges from the interaction of all 576 VQ tokens, but the autoregressive factorization decomposes this holistic signal into 576 per-token log-probability contributions, each individually uninformative about overall image quality. This decomposition is the fundamental mismatch between DPO’s token-factored objective and the global nature of visual preference.

J. Length-Controlled Understanding Evaluation

A potential confound in our understanding evaluation is that DPO might improve VQA scores by producing longer responses (which receive higher word-overlap scores) without generating more relevant content. To disentangle response quality from response length, we compute a *length-free* VQA score that removes length-dependent components (length bonus and short-response penalty) from the scoring function, retaining only word overlap with ground-truth captions ($\times 4.0$ weight) and novel content words (capped at 1.0).

Table 15. **Length-controlled understanding evaluation** (Janus-Pro-7B, $n=200$). The standard VQA score includes length components; the length-free variant removes them, retaining only word overlap and novel content words. Understanding-only DPO improves the length-free score by +0.15, confirming genuine content improvement (58% of the total gain), with only 42% attributable to length.

Method	VQA (std)	VQA (length-free)	Avg. words
Base model	2.490	1.932	53.7
Und-only DPO	2.753 (+0.26)	2.086 (+0.15)	63.1
Gen-only DPO	2.498 (+0.01)	1.946 (+0.01)	53.0
Naive Joint	2.485 (-0.01)	1.930 (-0.00)	53.1
PCGrad	2.508 (+0.02)	1.949 (+0.02)	53.7
Grad-Weighted	2.504 (+0.01)	1.935 (+0.00)	55.6
Length-Norm	2.532 (+0.04)	1.953 (+0.02)	56.6
Fixed-Weight	2.523 (+0.03)	1.946 (+0.01)	57.4

Analysis. Response length correlates with the standard VQA score ($r = 0.65$ for the base model), confirming that the length-free decomposition is informative. Understanding-only DPO produces responses averaging 63.1 words (vs. 53.7 for the base model), and 42% of its VQA improvement traces to longer responses. The remaining 58% (+0.15 length-free) reflects genuine content improvement: DPO-aligned responses contain more entity-relevant words that match ground-truth captions. Multi-task methods show smaller length increases (+1.9 to +3.7 words) and correspondingly smaller length-free improvements (+0.00 to +0.02), consistent with the understanding signal being partially drowned out by the larger generation gradient.